Auger-driven Motion in Granular Media

Stephanie L. Chang and Paul B. Umbanhowar

December 8, 2017

Abstract

The purpose of this project was to create an underground locomotor capable of following user-defined, arbitrary trajectories. Using FDM 3D printing, numerous iterations of a modular robot mounted with an auger were fabricated. Rapid, empirical tests within a loosely packed bed of poppy seeds were performed to clarify how certain auger parameters influenced the behavior of the robot in the horizontal plane. A theoretical model was derived to describe how the parameters of an auger and granular material characteristics can affect the amount of propulsive force generated.

Contents

1 Introduction

Why this project is interesting and important for the industry today Goal underground locomotor follow arbitrary trajectories Many geometries tried Maladen, push me pull me, etc.

2 Approach

Description on how I intended to build and test a robot in poppy seeds and created a mathematical model based off of Francisco's recent paper to optimize the parameters. Wings to counteract torque.

Initial idea to make and try.

Describe why we built it as it was and why we decided not to go with certain designs like the double screw. Modular for easy assembly and localized testing.

3 Iteration Progression

The robot consists of 5 main components. When powered, an Archimedes screw mounted at the head of the robot will spin to part granular media and pull the robot forward. This is attached to an adapter plate which fits snugly around the shaft of a DC motor. A cylindrical cap on the motor itself stops granules from falling into an exposed gear box. Wedged inside the protective cap are wings which prevent the body of the robot from rotating with the screw. Lastly, an elongated hemispherical housing unit covers the back of the robot to shield soldered wire junctions from wear and tear. Note, a modular robot was created to make testing different combinations of screws and wing shapes easier.

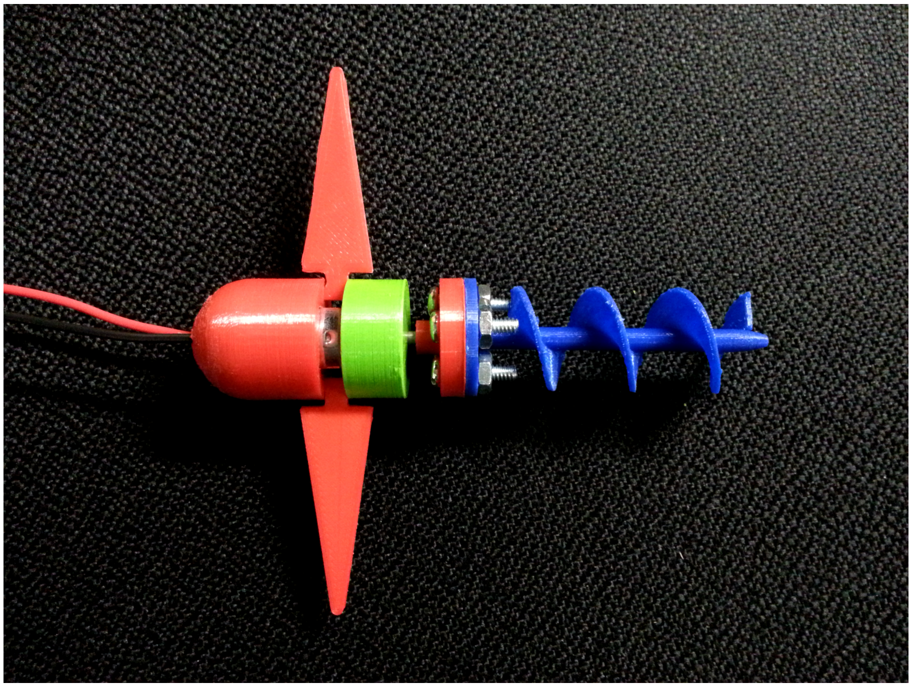

Figure 1: The first prototype of the augerbot

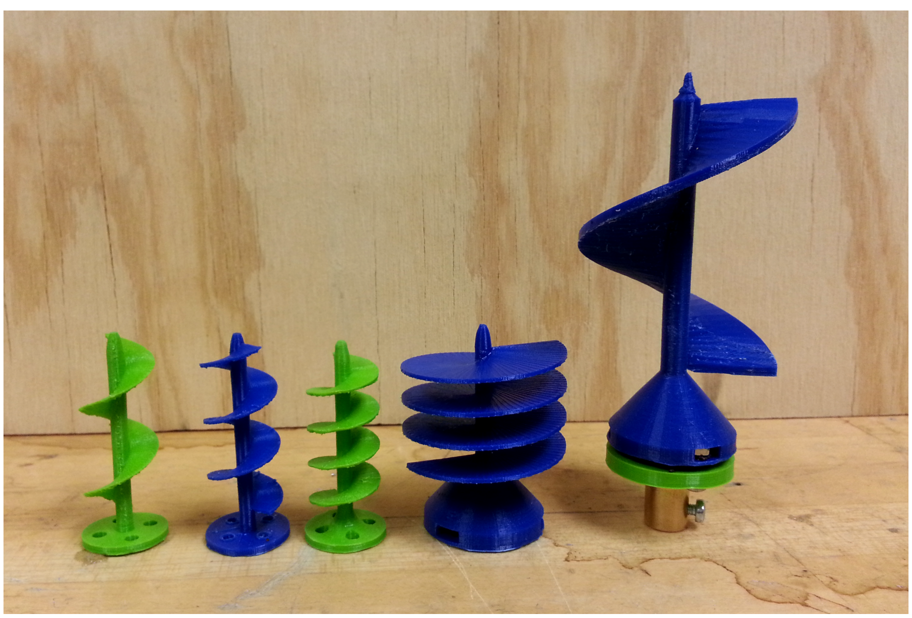

Figure 2: All augers tested

Describe what was seen with the first blind test. Problems encountered. How the following iterations were changed to compensate. Wider screw, modular wings, captured nuts for easier assembly and better interfacing with adapter, brass adapter for motor shaft to counter wt imbalance and keep the screw on since the PLA kept wearing after a while.

4 Analytical Optimization

During testing, screws with larger radii and pitches appeared to produce more propulsive force. To find the optimal parameters needed to maximize an auger's pulling ability, a more principled method - inspired by extant studies - was developed [1, 2].

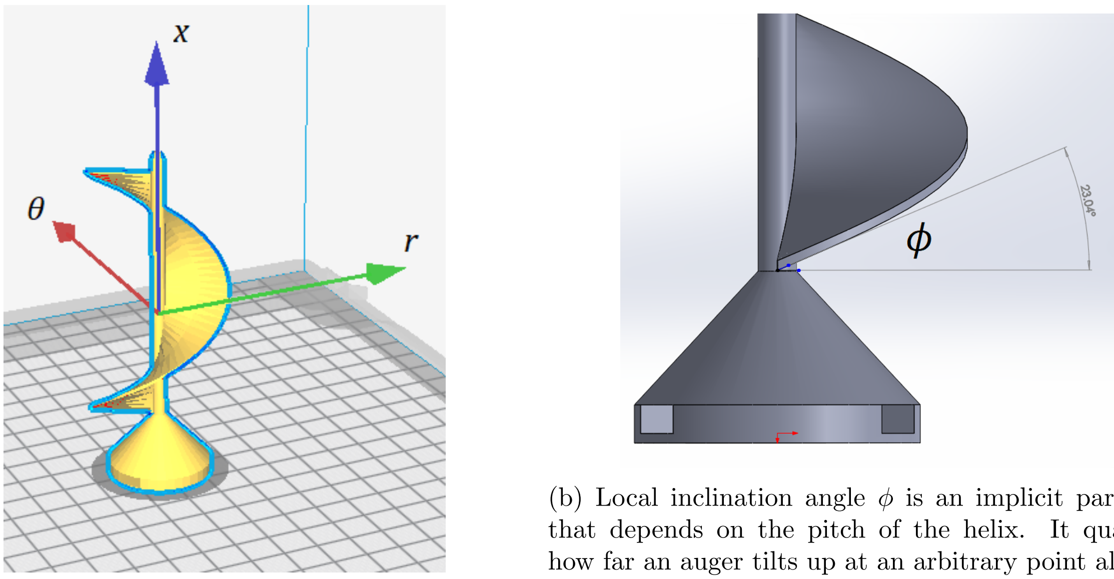

(a) The body coordinate system

(b) Local inclination angle ϕ is an implicit parameter that depends on the pitch of the helix. It quantifies how far an auger tilts up at an arbitrary point along its perimeter.

Figure 3: General problem set-up shown on an auger

A cylindrical coordinate system $(\vec{e_r}, \vec{e_\theta}, \vec{e_x})$ was used to describe the helix [Figure 3a]. Local inclination angle ϕ, shown in Figure 3b, was used to define tangential unit vector $\vec{e_t} = \langle 0, \cos(\phi), \sin(\phi) \rangle$ and normal unit vector $\vec{e_n} = \langle 0, \sin(\phi), -\cos(\phi) \rangle$. For a tiny segment along the helix path, the local velocity was determined to be $\vec{\nu} = \langle 0, rw, U \rangle$, where U refers to the translational velocity along the auger's x-axis. Algorithm 1 lists the steps which were taken to find ϕ_{opt} for a screw with a known radius R and number of revolutions n. Note, the auger's radius and height were restricted to account for the dimensions of the poppy seed tank and the build volume of the Ultimaker 3 3D printer.

Algorithm 1 Helix Local Inclination Optimization

Knowns:

R, n, d, ω ▷ Auger radius, number of turns, auger depth, and angular velocity
$0 < \varepsilon \ll 1$
$F_x(\phi, U)$ ▷ Propulsive force generated in the horizontal direction

Compute: Maximum helix translational velocity U for different ϕ values

```
Calculate C_n and C_t                                  ▷ Normal and tangential friction coefficients
Let φ = 10 * π/180
while φ < 90 * π/180 do
    U_guess = ε                                        ▷ Initialize the helix's x-direction velocity close to 0
    while F_x(φ, U_guess) > ε do                       ▷ Modified Newton-Raphson*
        U_guess = U_guess − F_x(φ, U_guess) / (d/dU F_x(φ, U_guess))
    end while
    Store φ and U_guess
    φ = φ + (1 * π/180)                                ▷ Increment φ by 1 degree
end while
Find the φ which corresponds to the largest U_guess saved
```

*Omitting the absolute value operator ensures that Newton-Raphson will not be employed to solve for the U-intercept when the line tangent at U_{guess} crosses the U-axis at a value ≤ 0. This is necessary because function $F_x(\phi, U)$ contains natural log terms.

Imagine an auger is composed of infinitesimal segments, each of which feels drag and thrust. According to resistive force theory (RFT), the amount of force generated by a body moving through granular media can be approximated by adding the forces experienced by each of its finite elements. $F_x(\phi, U)$, therefore, is the linear superposition of all local forces projected onto the x-axis. Mathematically, this calculation looks like

$$F_x(\phi, U) = \int_0^R \int_0^{2\pi n} (\vec{f} \cdot \vec{e_x}) \frac{r}{\cos(\phi)} d\theta dr \ , \tag{1}$$

where $\vec{f}$ denotes the force per unit area felt by each partition. Coulomb's law of friction was used to express $\vec{f}$ as the sum of two force components tangential and normal to stem of the auger. Fleshed out, this equation takes the form

$$\begin{aligned} \vec{f} &= -C_t(\vec{e_\nu} \cdot \vec{e_t})\vec{e_t} - C_n(\vec{e_\nu} \cdot \vec{e_n})\vec{e_n} \\ &= \frac{-C_t(rw\cos(\phi) + U\sin(\phi))\vec{e_t} - C_n(rw\sin(\phi) - U\cos(\phi))\vec{e_n}}{\sqrt{U^2 + (rw)^2}} \ , \end{aligned} \tag{2}$$

where C_t and C_n represent depth- and ϕ- dependent tangential and normal stress coefficients respectively.

Plugging equation (2) into equation (1), the total amount of propulsive force generated by the auger in the x-direction was found to be

$$\begin{aligned} F_x(\phi, U) = \frac{2\pi n}{\cos(\phi)} \Bigg[&(C_n - C_t)\omega \sin(\phi)\cos(\phi) \left(\frac{R}{2\omega^2}\sqrt{(R\omega)^2 + U^2} + \frac{U^2}{2\omega^3} \left(\ln \frac{U}{R\omega + \sqrt{(R\omega)^2 + U^2}} \right) \right) \\ &- \frac{U}{\omega^2}(C_t \sin^2(\phi) + C_n \cos^2(\phi)(\sqrt{(R\omega)^2 + U^2} - U) \Bigg] \end{aligned} \tag{3}$$

where $\vec{e_x} = \langle 0, 0, 1\rangle$. Introducing non-dimensional helix velocity $\tilde{U} = \frac{U}{R\omega}$, equation (3) was rearranged as follows

$$F_x(\phi, \tilde{U}) = \frac{2\pi R^2 n}{\cos(\phi)} \left[\frac{1}{2}(C_n - C_t)\sin(\phi)\cos(\phi) \left[\sqrt{1+\tilde{U}^2} + \tilde{U}^2 \ln\left(\frac{\tilde{U}}{1+\sqrt{1+\tilde{U}^2}} \right) \right] - \tilde{U}(C_t \sin^2(\phi) + C_n \cos^2(\phi)) \left(\sqrt{1+\tilde{U}^2} - \tilde{U} \right) \right] . \tag{4}$$

When the system is at equilibrium, ϕ is the only parameter that controls the value of U. Recall, C_t and C_n both depend on ϕ. The steady-state case is important because, when thrust and drag are balanced, U is the constant velocity at which the auger advances along the x-direction. Algorithm 1, therefore, systematically varies $\phi \in \left(0, \frac{\pi}{2}\right]$ to find the ϕ_{opt} value which yields the highest U.

If an auger is placed on its side, small segments along the body can be interpreted as tiny plates [Figure 4]. Regardless of its location around the x-axis, the attack angle β of each segment is the same. With this in mind, C_t and C_n were determined using fitting functions proposed by Chen *et al.* For a prone helix translating axially within loosely packed poppy seeds ($\gamma = 0$) these force coefficients were computed using

$$C_t = [0.02\sin(-2\beta) + 0.051 + 0.047\cos(2\beta) + 0.053\sin(2\beta)]\, d \tag{5}$$

and

$$C_n = [0.057 + 0.025\sin(2\beta) - 0.026\cos(2\beta)]\, d \ , \tag{6}$$

where d is a known depth.

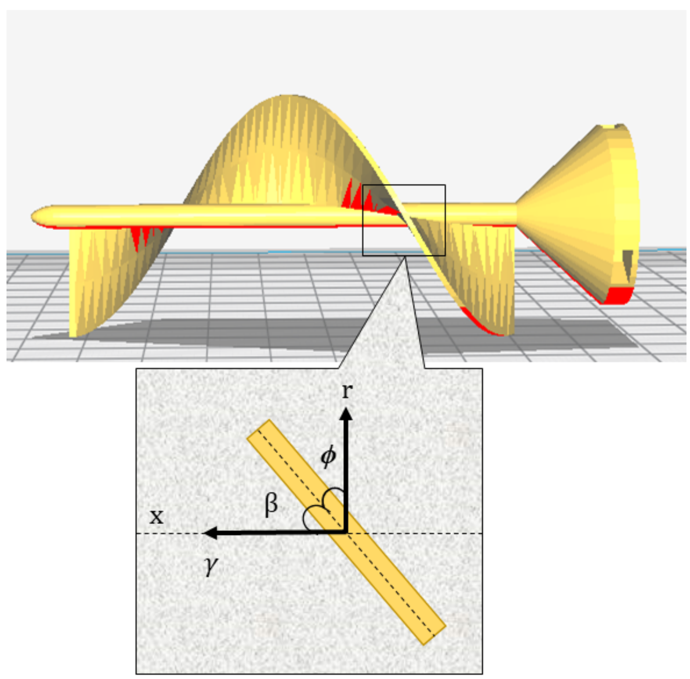

Figure 4: A plate element moving through granular media. Attack angle $\beta = \frac{\pi}{2} - \phi$ sets the tilt of the plate with respect to the horizontal plane. Intrusion angle γ defines the direction the plate moves with respect to the horizontal plane.

With explicit equations known for $F_x(\phi, U)$, C_t, and C_n, an aggressive auger was designed by first setting $R = 0.02\,\text{m}$ and $n = 1$. These values were arbitrarily chosen since R and n do not influence U

when drag and thrust are balanced. Algorithm 1, using equations (3, 5-6), was then implemented to predict U for different values of ϕ [Figure 5].

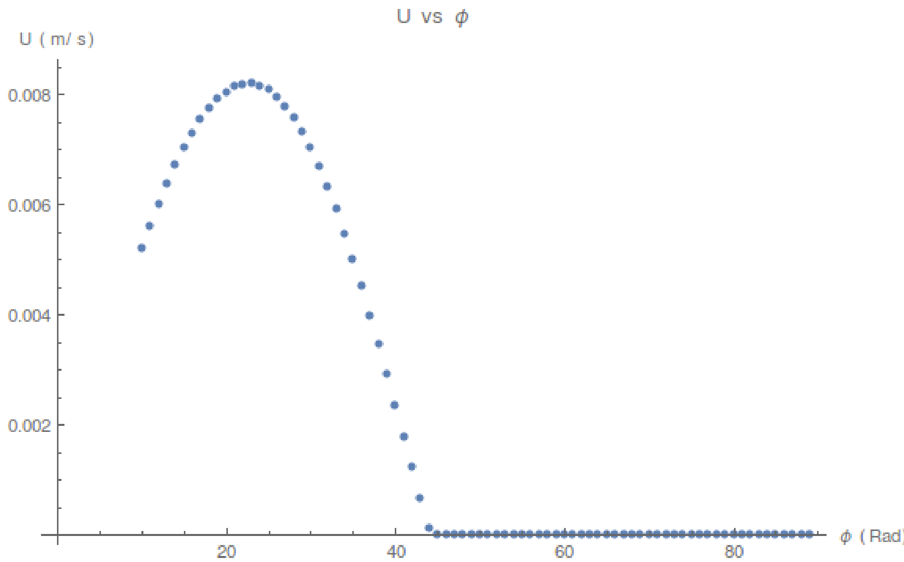

Figure 5: U (m/s) vs. ϕ (rad) for a prone auger ($R = 0.02\,\mathrm{m}$, $n = 1$, and $\omega = 3.51\,\frac{\mathrm{rad}}{\mathrm{s}}$) moving in the x-direction buried at a depth of $d = 0.05\,\mathrm{m}$ in loosely packed poppy seeds. ϕ was varied from $10°$ to $90°$ in increments of $1°$.

As shown above, the maximum value of U ($8.197\,36 \times 10^{-2}\,\frac{\mathrm{m}}{\mathrm{s}}$) occurs when $\phi = \phi_{opt} = 23°$.

To check if algorithm 1 was formulated correctly, the velocity of a thin wire coil in the x-direction was modeled using ϕ-dependent friction coefficients [2]. When $R_{wire} \ll R_{helix}$,

5 Optimized Augerbot Results and Analysis

According to the optimization results, an auger with a radius of $0.02\,\mathrm{m}$, one turn, and a local inclination angle of $23°$ was fabricated [Figure 6].

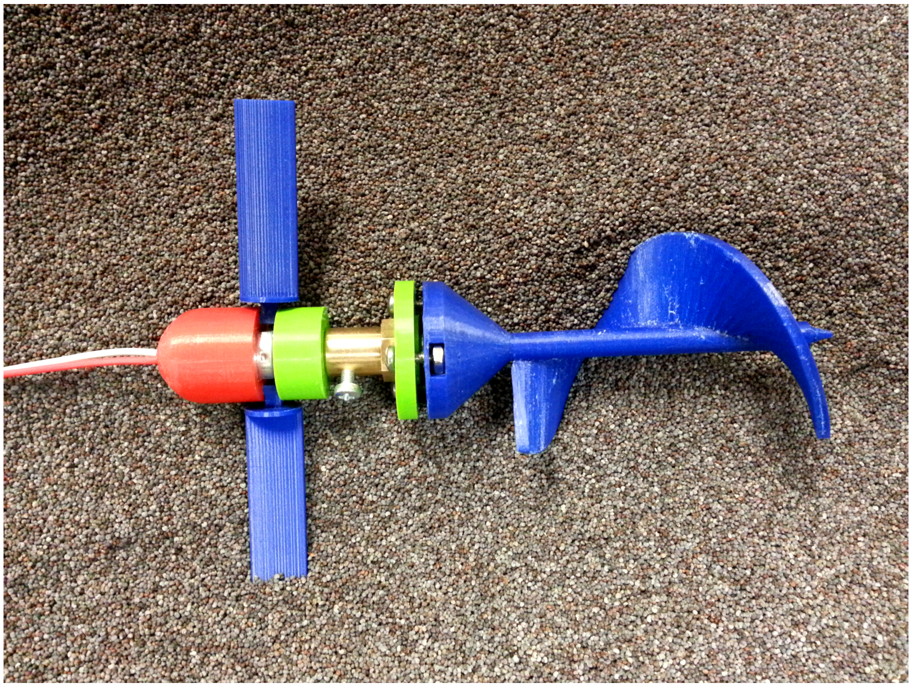

Figure 6

Describe results with math model. Implementation of Francisco's model with Chen's coeff Our full Fx model with...whatever coeff end up being proper

limitations with printer

Speculate all the things as to why things failed or not?

6 Future Direction

Future direction larger wings, fatter wings wings with opposite angles to counter cw bias

References

[1] Baptiste Darbois Texier, Alejandro Ibarra, and F Melo. Helical locomotion in granular media. 119, 07 2017.

[2] Chen Li, Tingnan Zhang, and Daniel I. Goldman. A terradynamics of legged locomotion on granular media. *Science*, 339(6126):1408–1412, 2013.